Supporting Information for

Axial Nanometer Distances Measured by Fluorescence Lifetime Imaging Microscopy

Michael Berndt,[†] Mike Lorenz,[†] Jörg Enderlein,[‡] and Stefan Diez [†]

[†] *Max-Planck-Institute of Molecular Cell Biology and Genetics, 01307 Dresden, Germany.*

[‡] *III. Institute of Physics, Georg-August-University, 37077 Göttingen, Germany.*

Supporting Methods

Microtubule preparation. Microtubules are polymerized from tubulin (8 mg/ml) labeled with Alexa Fluor 488 (80% labeling ratio) or labeled with Alexa Fluor 488 and functionalized with biotin (60% labeling ratio, and 6.25% biotinylation ratio) in BRB80 buffer (80 mM PIPES, 1 mM EGTA, 1 mM $MgCl_2$, pH 6.9) supplemented by 4 mM $MgCl_2$, 5% DMSO in water and 1 mM GTP to a final volume of 6.25 μL. After incubation for 1 hour at 37 °C the polymerized microtubules are stabilized by diluting into BRB80 containing 10 μM taxol (BRB80T), to a final volume of 400 μL. The solution is centrifuged for 5 min at 134,000×g. The resulting pellet is re-suspended in 100 μL of BRB80T. Microtubules, with biotinylated centers only, are polymerized in two steps, following a protocol for polarity-marked microtubules[1]: The centre is polymerized from a mixture of Alexa Fluor 488 labeled and biotinylated tubulin (concentration, labeling and biotinylation as above) and incubated for two hours at 37 °C with 1 mM GMPCPP, 1 mM $MgCl_2$ and BRB80 buffer at a final volume of 50 μL. After the centrifugation step (see above) and resuspension in 12 μL of BRB80, these microtubule seeds are added to the first mentioned polymerization mix containing Alexa Fluor 488 labeled tubulin (80% labeling ratio) to continue the polymerization on both ends of the microtubule seed.

Microtubule assays. Experiments are performed in a microscope flow cell consisting of two microscope cover glasses (22 mm^2 at the bottom, 18 mm^2 at the top, #1.5, zinc-titania glass, Corning Inc., Corning, USA), sandwiched and held together by double-sided tape (Scotch 3M, St. Paul, USA) forming accessible channels. The bottom cover glass is coated with a thermally evaporated gold surface of 15 nm thickness with a 1 nm adhesion layer of titanium beneath (PVD-Beschichtungen, Silz, Germany), which is oriented to the inner side of the flow cell (see Fig. 1). Microtubules are then immobilized at different elevation levels above the gold surface in the flow cell. For the avidin-fixed microtubule experiments, a diluted microtubule solution is flowed into the flow cell. Allowing the microtubules to settle for 5 min, results in some microtubules loosely adhering to the surface. To prevent microtubule bundling, only then a 1 μM avidin solution (Sigma-Aldrich) is flown in. The avidin forms a layer between microtubules and the flow cell by electrostatic interactions and immobilizes the previously loosely adhered microtubules. Both solutions contain anti-fade reagents (20 mM D-glucose, 0.04 mM glucose oxidase, 0.01 mg/ml catalase and 10 mM DTT) to prevent photo-bleaching and photo-oxidation. For the neutravidin-coated avidin-fixed microtubules, biotinylated microtubules are kept for 5 min in 100 μM neutravidin solution, allowing the neutravidin to bind to the microtubules before flowing into the flow cell and immobilizing them with avidin as described above. The experiments with the microtubule-kinesin system are prepared by immobilizing gliding microtubules on a kinesin-1 coated gold surface: A solution containing casein (0.5 mg/ml in BRB80) is flowed into the flow cell and incubated for 5 min before the motor solution (7.5 μg/ml kinesin-1, full-length, conventional kinesin-1 from *Drosophila melanogaster*[2], 0.4 mM Mg-ATP, 0.2 mg/ml casein, 10 mM DTT in BRB80) is flowed in. After another 5 min, the motor solution is exchanged with a motility solution containing microtubules and 0.2 mM ATP. After sufficient time, to allow binding of the microtubules to the kinesin-1 molecules on the surface, the motility solution is replaced by the same solution but without microtubules in order to limit the number of microtubules binding to the kinesin. Subsequently the motors are stalled with a solution containing 1 mM AMPPNP a non-hydrolysable ATP analogue. The last three solutions also contain the anti-fade mix. For measurements in free solution, microtubules are

immobilized in geometries distant from a surface. Here, a 0.5% low-melt agarose solution (Invitrogen, Carlsbad, USA) is used together with the microtubules and the anti-fade solution (10 mM D-glucose, 0.02 mM glucose oxidase, 0.005 mg/ml catalase and 5 mM DTT). The buffer for all solutions is BRB80T.

Experimental Setup and Data Acquisition. Fluorescence lifetime measurements are performed on a wide-field time-domain fluorescence lifetime imaging microscope (FLIM) (see Fig. 1). As an excitation light source a Chameleon XR Ti:Sapphire Laser (Coherent, Santa Clara, USA) with 200 fs pulses and a repetition rate of 90 MHz is tuned to 980 nm and frequency doubled to 490 nm using a second-harmonic generator (APE, Berlin, Germany). Finally, the laser beam is coupled into a liquid light guide fiber (Newport, Irvine, USA), expanded with a collimator, and coupled into the microscope. Images are recorded on a Zeiss Axiovert S100TV (Zeiss, Oberkochen, Germany) with a 63x c-apochromat water-objective (NA 1.2, correction collar) (Zeiss, Oberkochen, Germany) through an FF500-Di01 dichroic mirror and a BL HC536/40 emission band-pass filter (both Semrock, Rochester, USA). The water objective is used to avoid aberrations caused by focusing through the aqueous solution in the flow cell. The refractive index of the aqueous solution is determined with a refractometer to n=1.3384 (AR4D, Krüss, Hamburg, Germany). The images are acquired at the microscope's bottom port with an intensified PicoStar HR 12 camera system (LaVision, Göttingen, Germany). The time-gated image intensifier is triggered directly by the laser trigger through a programmable picosecond-trigger-delay unit (LaVision, Göttingen, Germany). The microscope is fully automated and controlled with custom-written software (LabView 8.2, National Instruments, Austin, USA). Images are acquired and analyzed with the same software. Further information on the setup can be found in[3,4].

The fluorescence decay is obtained from a time-series of 18 wide-field images recording the intensity of the sample at different time points after excitation by the femtosecond laser pulses. These

images are taken with a gate width of 1000 ps and a delay time of 500 ps in between. The camera is set to a 4x4 binning and an exposure time of 500 ms for each image. With the chosen settings, the pixel size of the camera is 850 nm x 850 nm. The laser power can be adjusted by neutral density filters to avoid photo-bleaching during the acquisition.

Supporting Discussion

Data analysis. From the recorded fluorescence decay time-series, fluorescence lifetime values (τ) of microtubules held by various spacer molecules above the gold surface are calculated for each pixel by fitting the intensities according to $I = A \cdot e^{-t/\tau} + c$, with I being the measured intensity at a time point t, the pre-exponential factor A, and a constant offset c. Only pixels are fitted, which carry signal, i.e. in which microtubules are visible. The temporal range of the image series incorporated into the lifetime fit is chosen such that: *(i)* the first image does not temporally overlap with the excitation laser pulse (tail-fitting) and *(ii)* incorporation of the last image does not lead to an overestimation of the lifetime due to noise along the tail of the exponential decay.

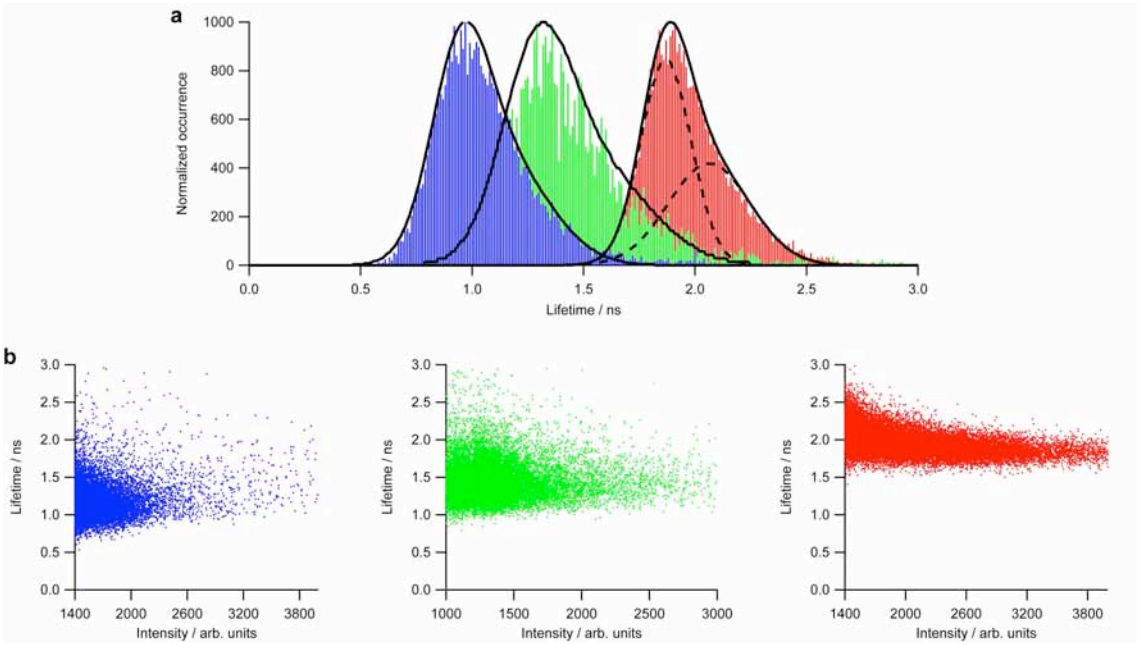

Supporting Figure 1 - Details on data analysis.

Histograms of the lifetime distributions and intensity-lifetime correlation plots obtained from the three experiments pictured in Fig. 2 (blue – microtubules avidin-fixed, green – neutravidin-coated, avidin-fixed microtubules, red – microtubule-kinesin).

(a) Histograms reveal two Gaussian components with different means (black solid lines). The superposition of both Gaussian functions is shown by the black dashed lines (for the microtubule-kinesin system).

(b) The lifetime-intensity correlation plots of the above measurements reveal that the second (longer) lifetime component originates from low intensities, which correspond to pixels at the microtubule rims and are hence discarded in the analysis.

The results obtained in each measurement are visualized as lifetime images by color-coding the lifetime of each pixel (e.g. in Fig. 2) and plotted in a histogram for quantitative evaluation displaying lifetime vs. occurrence (Supporting Figure 1a). For uncorrelated data one would expect the histogram to follow a normal distribution, described by a single Gaussian function[5]. However, we find that the lifetime distributions displayed in the histogram are described by a superposition of two Gaussian functions with means at different lifetimes. The double-Gaussian is the result of an existing correlation between lifetime and intensity, which is shown in the correlation plots (Supporting Figure 1b); data derived from pixels with lower intensity values are biased towards longer lifetimes. We found, that

these pixels spatially correspond to the outer edges of the microtubules in the image, where the measured fluorescence intensity only partially results from fluorescent microtubules but rather contains a substantial amount of additional noise. We therefore discard the lifetime determined by this component of the double-Gaussian function and determine the fluorescence lifetime of one particular experiment only from the pixels, which do not show any correlation between lifetime and intensity. These are pixels found along the centerlines of the microtubules.

One can avoid the occurrence of the artificial second Gaussian at higher lifetimes without changing the results by initially setting a threshold at which data are evaluated. In fact, evaluating thresholded data leads to the same results. However, for an unbiased evaluation of data, it is recommended to analyze the entire dataset, before initial rejection of parts of them.

All lifetime values are checked additionally by an independent method, where the intensities of all pixels in a region-of-interest are summed up before exponential fitting. The values obtained from both methods do not differ more than 10%.

Regarding the accuracy, we have identified the lifetime-fitting procedure to be the most susceptible part to errors in our setup. However, obtained lifetimes change at maximum ±0.15 ns upon extending or reducing the number of selected images incorporated into the fitting range. Given the high linearity of the slope of the model curve (Fig. 2d) in the range from 0 nm to about 40 nm, the error converts to a fitting error of about ±3 nm.

Modeling. The CPS model describes an emitting dye molecule as an ideal electric dipole oscillator and calculates its interaction with a metal layer on the basis of Maxwell's equations of electrodynamics. Finally, it interprets the emission rate of the dipole in terms of an observable fluorescence lifetime.

The modeling of the observed reduction of the fluorescence lifetime is performed in several steps: First the emission energy flux (length of the Poynting vector) of a single dipole emitter is calculated as a distance- and wavelength-dependent function of emitter orientation with respect to the gold surface[6,7,8], which is described by its dielectric function experimentally determined by ellipsometry

(Supporting Figure 2). For the model, one has to add the emission energy flux through the metal/water interface (below the emitter) and the emission energy flux through a planar interface above the emitter (virtual water/water interface).

For the emission energy flux through the water/metal interface, one can find the expressions for a horizontally and vertically oriented dipole with *unity* quantum yield of fluorescence and *unity* dipole amplitude (in cgs unit system)

$$S^0_{\parallel,-}(z,\lambda) = \frac{ck_0^4}{4}\left\{\int_0^{n_1} dw \ \frac{n^2-w^2}{n^2}\left(1-\left|R_p^2\right|\right) + 2\int_0^{\infty} dw \frac{n^2+w^2}{n^2} \ \mathrm{Im}\ R_p e^{-2k_0 wz}\right\}$$

and

$$S^0_{\perp,-}(z,\lambda) = \frac{ck_0^4}{8}\left\{\int_0^{n_1} dw \ \left[\frac{w^2}{n^2}\left(1-\left|R_p^2\right|\right) + \left(1-\left|R_s^2\right|\right)\right] + 2\int_0^{\infty} dw \left[\frac{w^2}{n^2}\mathrm{Im}R_p - \mathrm{Im}R_s\right] e^{-2k_0 wz}\right\}$$

For the emission energy flux through a virtual interface in water above the emitter one finds

$$S^0_{\parallel,+}(z,\lambda) = \frac{ck_0^4}{4}\int_0^{n_1} dw \frac{\left(n^2-w^2\right)}{n^2}\left|1+R_p e^{2ik_0 wz}\right|^2$$

and

$$S^0_{\perp,+}(z,\lambda) = \frac{ck_0^4}{8}\int_0^{n_1} dw \left[\frac{w^2}{n^2}\left|1-R_p\, \mathrm{e}^{2ik_0 wz}\right|^2 + \left|1+R_s e^{2ik_0 wz}\right|^2\right].$$

In these equations, the following symbols have been used: *c* denoting the speed of light, k_0 is the length of the wave-vector in vacuum, i.e. $k_0 = 2\pi/\lambda$, *w* is the component of the wave vector in water, normal to the interface divided by k_0, *n* is the refractive index of water, and the $R_{p,s}$ are the incidence-angle dependent (and thus *w*-dependent) total reflection coefficients for planar *p*- and *s*-waves at the metal/water interface taking the whole configuration of the water/metal layer/glass stack into account. These coefficients are found using propagation matrices for the electric field through all interfaces and layers.

Hence, the total emission energy flux of the emitter is given by

$$S^0_{\|,\perp}(z,\lambda) = S^0_{\|,\perp,+}(z,\lambda) + S^0_{\|,\perp,-}(z,\lambda).$$

All equations are normalized in such a way that the total emission energy flux of a free dipole in water (no interfaces) is equal to $S^0_{free} = ck_0^4 n/3$. Thus, for an emitter with unity quantum yield, the ratio of its emission rate $k^0_{\|,\perp}$ in the presence of metal layer and glass support to its free emission rate in water k^0_{free} is given by the ratio of $S^0_{\|,\perp}$ to S^0_{free}, i.e. emission rates and emission energy flux are similar up to a proportionality constant.

Taking the real (i.e. non-unity) quantum yield of the dye q_f into account, the transition rates are given by

$$k_{\perp\|}(z,\lambda) = [q_f \frac{S^0_{\perp\|}(z,\lambda)}{S^0_{free}} + 1 - q_f]k^0_{free}$$

The emission rate has next to be averaged over all possible orientations and all emission wavelengths weighted with the free emission spectrum of the dye. Assuming an isotropic orientation distribution of the dipole emitters, orientation averaging is approximated by taking the arithmetic mean of the vertical orientation and two times the horizontal orientation. Averaging over all emission wavelengths is carried out by using the free *normalized* emission spectrum $F(\lambda)$ of the dye. Thus, one arrives at

$$\bar{k}(z) = \int_{\lambda_1}^{\lambda_2} d\lambda F(\lambda) \frac{k_\perp(z,\lambda) + 2k_\|(z,\lambda)}{3}$$

where λ_1 and λ_2 are the limits of the spectral range transmitted by the filters in the detection path. Finally, one has to take into account the finite size of the microtubules (assumed to be homogeneously labeled). This is done by averaging the emission rate over all fluorophore positions around a vertical circle with a radius corresponding to the radius of a microtubule (12.5 nm). Here, one peculiarity has to

be taken into account: fluorophores at different distances from the gold surface show not only different lifetimes, but also different observable intensities due to different fluorescence quenching rates. The observable fluorescence intensity is inversely proportional to the emission rate as given by the preceding equation. Also, for each fluorophore, the observable lifetime is inversely proportional to its emission rate. Thus, after averaging over all fluorophore positions around the vertical circle, the finally observable mean lifetime is given by the average

$$\bar{\tau}(z_b) = \left[\oint_{circle} dz \bar{k}^{-2}(z) \right] \Big/ \left[\oint_{circle} dz \bar{k}^{-1}(z) \right]$$

where z_b denotes the bottom position of the circle.

In general, the CPS model requires following input parameters: *(i)* the dielectric function of the 15 nm gold film at the wavelength used, *(ii)* the quantum yield of the dye labeled molecules in free solution (i.e. not perturbed by any surface) (measurement see Supporting Experiments) and *(iii)* the free emission spectrum of the dye. Once computed for the fluorescent probes used, the obtained lifetime-distance relations can be consecutively used in each measurement.

Supporting Experiments

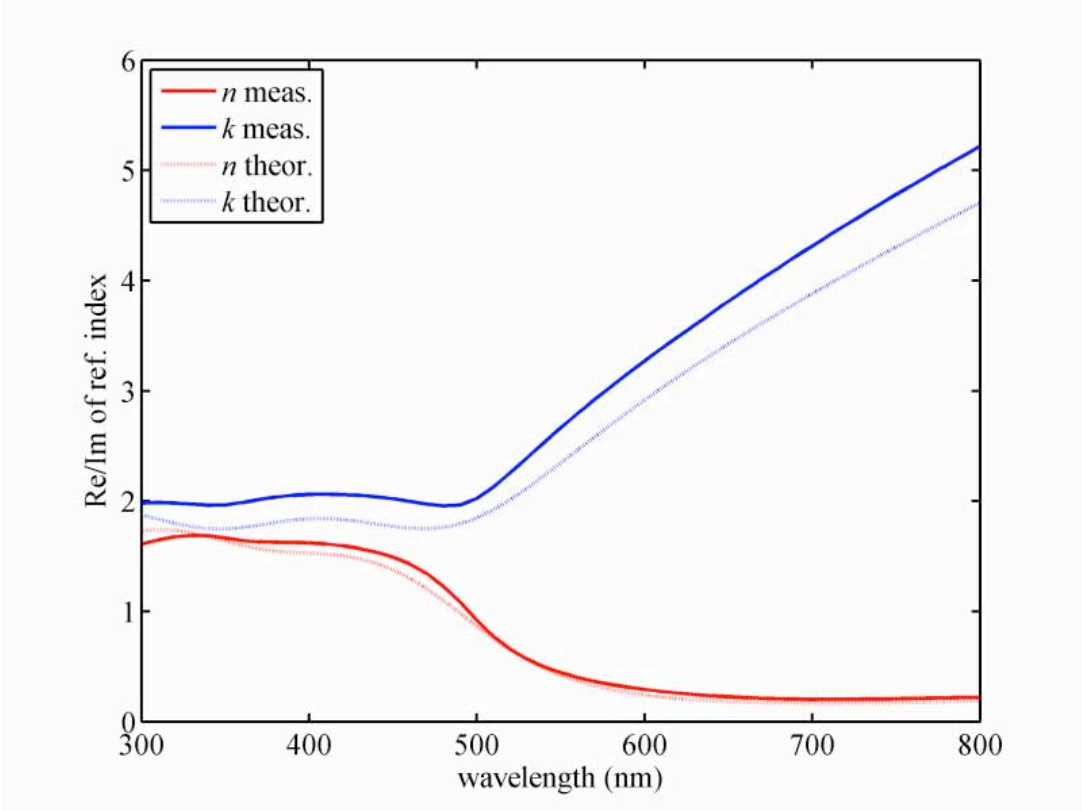

Supporting Figure 2 – Dielectric function of the gold films used.

Dispersion of the dielectric function $\varepsilon(\lambda) = n(\lambda) + ik(\lambda)$ of a 15 nm gold surface coated on glass as used in the experiments. The solid curves represent the values measured with ellipsometry, the dashed-light curves represent the theoretical (ideal) values of a smooth gold film of 15 nm thickness[9]. Ellipsometry yields the thickness of the experimentally used gold surface to 14.6 nm. The low deviation between experimental and theoretical values indicates an almost perfect description of the gold surface by a smooth film, indicating the negligible roughness of the gold surface.

Supporting Table 1 - Control experiments

Lifetime values and s.e.m. obtained from the measurement of bright, dim, and defocused avidin-fixed microtubules. The dimly labeled microtubules possess only half the labeling ratio of the bright microtubules. The defocused microtubules are imaged with the microscope defocused 2 μm into the sample. Neither the lifetime obtained for the dim microtubules nor for the defocused microtubules differs significantly from the lifetime obtained for bright and focused microtubules.

	Bright & focused microtubules	**Dim & focused microtubules**	**Bright & defocused microtubules**
Measured lifetime	0.91±0.05 ns (n=24)	0.90±0.05 ns (n=5)	0.96±0.04 ns (n=6)

Determination of the quantum yield of Alexa Fluor 488 labeled microtubules. The fluorescence quantum yield of the microtubule-bound Alexa Fluor 488 is calculated according to

$$\frac{Q}{Q_{ref}} = \frac{I \cdot OD_{ref}}{I_{ref} \cdot OD} \cdot \frac{n^2}{n_{ref}^2}$$

where Q is the quantum yield, I the integrated fluorescence intensity, OD the optical density, and n the refraction index. The subscript *ref* refers to a reference fluorophore of known quantum yield.

As reference, fluorescein (Sigma-Aldrich, St. Louis, Missouri, USA) in 0.1 N NaOH with Q_{ref}=0.92 is used[10]. The optical density of both solutions is measured on a NanoDrop 1000 (Thermo Scientific, Waltham, Massachusetts, USA) and is below 0.02. The full fluorescence spectra are recorded with an μL-cuvette on a FluoroMax-3 (Jobin Yvon Horiba, Oberursel, Germany) from 460 nm to 700 nm with an excitation wavelength of 450 nm. To avoid polarization artifacts all measurements are done under magic-angle conditions. Finally, the total fluorescence intensity I is determined by integrating the fluorescence spectra from 475 nm to 695 nm. Both samples are measured in aqueous solution, hence slight differences in refraction indices are negligible. The quantum yield of Alexa Fluor 488 labeled microtubules is determined to 0.82±0.03. This agrees with the reduction of quantum yield observed by

the reduction of fluorescence lifetime of unbound compared to microtubule-bound Alexa Fluor 488 from 4.1 ns and Q=0.92[11] to 3.53±0.05 ns and Q=0.79±0.02, respectively.

Supporting References

1. Howard, J.; Hyman, A. A. *Methods in Cell Biology, Vol 39* **1993,** 39, 105-113.
2. Hancock, W. O.; Howard, J. *Journal of Cell Biology* **1998,** 140, 1395-1405.
3. Elangovan, M.; Day, R. N.; Periasamy, A. *Journal of Microscopy* **2002,** 205, 3-14.
4. Lorenz, M. *RNA* **2009,** 15, 97-103.
5. Young, H. D., *Statistical Treatment of Experimental Data* **1962**.
6. Chance, R. R.; Prock, A.; Silbey, R., *Advances in Chemical Physics* **1978,** Vol. XXXVII, 1-65.
7. Enderlein, J. *Biophysical Journal* **2000,** 78, 2151-2158.
8. Enderlein, J.; Ruckstuhl, T. *Optics Express* **2005,** 13, 8855-8865.
9. Rakic, A. D.; Djurisic, A. B.; Elazar, J. M.; Majewski, M. L. *Appl Optics* **1998,** 37, 5271-5283.
10. Demas, J. N.; Crosby, G. A. *J Phys Chem-Us* **1971,** 75, 991.
11. Molecular Probes, *The Handbook* **2009**.